Elimination of Thermally Generated Charge in Charged Coupled Devices Using Bayesian Estimator

Jan ŠVIHLÍK, Petr PÁTA

Dept. of Radio Electronics, Czech Technical University, Technická 2, 166 27 Praha, Czech Republic

svihlj1@fel.cvut.cz, pata@fel.cvut.cz

Abstract. *This paper deals with advanced methods for elimination of thermally generated charge in astronomical images, which were acquired by a Charged Coupled Device (CCD) sensor. There exist a number of light images acquired by telescope, which were not corrected by dark frame. The reason is simple: the dark frame doesn't exist, because it was not acquired. This situation may for instance come when sufficient memory space is not available. Correction methods based on the modeling of the light and dark image in the wavelet domain will be discussed. As the model for the dark frame image and for the light image the generalized Laplacian was chosen. The model parameters were estimated using moment method, whereas an extensive measurement on an astronomical camera was proposed and done. This measurement simplifies estimation of the dark frame model parameters. Finally a set of astronomical testing images was corrected and then the objective criteria for an image quality evaluation based on the aperture photometry were applied.*

Keywords

Dark frame correction, Bayesian estimator, discrete wavelet transform, generalized Laplacian.

1. Introduction

There exist many astronomical observatories on the world. These observatories produces huge amount of scientific image data, which are investigated by several researchers. Unfortunately, a large number of scientific images needs a sufficient storage memory space, even if they are suitably compressed. For instance, when the images of night sky acquired by CCD (Charge Coupled Device) sensor are considered then it is necessary to acquire among others also a correction dark frame beside a light image. This image serves for the thermally generated charge elimination, which is made by subtraction of the dark frame from the light image. The thermally generated charge can be also eliminated by nonlinear median filtering, but this method is not so satisfactory. The method described in this paper allows to correct the light image directly and among others saves a memory space.

2. Image Data

16 bits scientific astronomical images (fits and dat format) were chosen for the simulations. FITS (Flexible Image Transport System) is primarily designed to store scientific data sets. These scientific analyzed data has been taken during the work of the international (Czech-Spanish) experiment BOOTES (Burst Observer Optical Transient Exploring System). The BOOTES [1] has been in service since 1998 as the first Spanish robotic telescope for the sky observation.

Fig. 1. The 1m11.01.dat image, exposure time = 300 sec, CCD temperature = 4.21 °C.

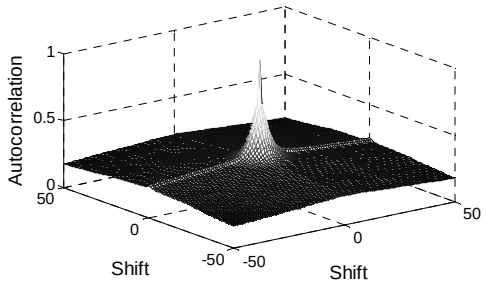

Fig. 2. The 1m11.01.dat image autocorrelation function.

This system is one of three similar systems in fully operation in the world. The main aim of the project is an observation of the extragalactic objects and detection of a new optical transient (OT) of gamma ray burst (GRB) sources. An example of the light image is depicted in Fig. 1. An image behavior can be described using autocorrelation function. There is a typical autocorrelation function of the astronomical images in Fig. 2; the shape of this autocorrelation function is quite slim. This means that astronomical

images are noise similar. The z axis shift of the autocorrelation denotes the direct-current component.

3. Discrete Wavelet Transform

The following items will deal with several type of DWT. Firstly the algorithm proposed by Stefan Mallat [2], which is called Dyadic Decomposition, will be mentioned. Mallat's nonredundant algorithm is based on the iterative filter bank. The consequent algorithm, e.g. Undecimated Wavelet Transform, is the redundant decomposition. The redundant decompositions are usually used for denoising, because of good efficiency.

3.1 Dyadic Decomposition

A dyadic decomposition was used as a special form of The Discrete Wavelet Transform in this work [3]. A dyadic decomposition allows non redundant decomposition of signal (in contrast to Continuous Wavelet Transform - CWT).

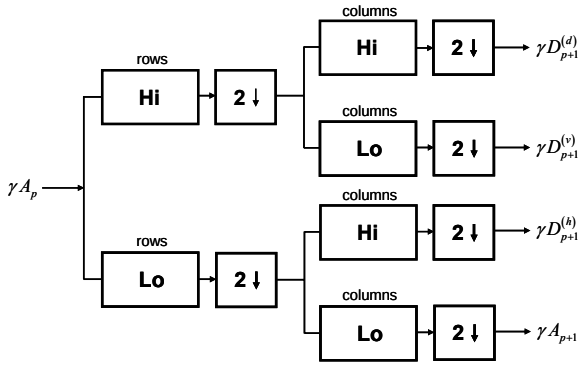

Fig. 3. The implementation of 2-D dyadic decomposition.

There is a basic structure for dyadic decomposition in Fig. 3. Here *Hi* respectively *Lo* presents the impulse response of a high pass, respectively low pass filter, $2\downarrow$ means down sample by factor 2. When the signal is filtered using the scheme in Fig. 3 then the four subbands are obtained, e.g. diagonal details (HH) $\gamma D_{p+1}(d)$, vertical details (HL) $\gamma D_{p+1}(v)$, horizontal details (LH) $\gamma D_{p+1}(h)$ and signal approximation (LL) γA_{p+1}. It is good to note that γA_0 presents the decomposed signal.

Decomposition filters were estimated from the wavelet Coiflet4. This wavelet gives satisfactory denoising results in the sense of MSE (Mean Square Error) [4]. The decomposition of the typical astronomical image can be seen in Fig. 4.

3.2 Undecimated Wavelet Transform

The decimated versions of wavelet transform are usually used. Unfortunately these types of the transform can produce unwanted artifacts during the reconstruction. Because of this, Undecimated Wavelet Transform (UWT) was developed, see [5]. The UWT belongs to redundant decompositions and it is a good tool for image denoising.

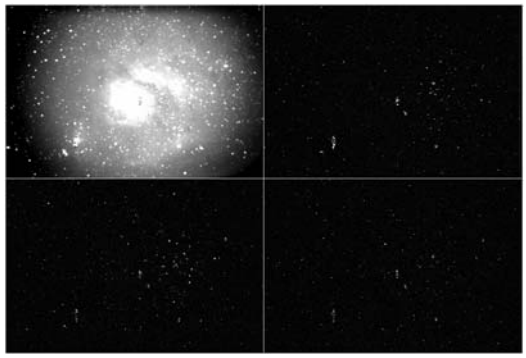

Fig. 4. Coefficients magnitudes of a dyadic decomposition of the light image, LL1 – top left, HL1 – top right, LH1 – bottom left, HH1 – bottom right.

4. Image Model

4.1 Light Image Model

Mallat as one of the first has observed that the DWT detail subbands have non-Gaussian statistics. Thus the detail subbands are characterized by a histogram, which is sharp peaked at zero with heavy tails. Mallat, Simoncelli [6] and others have modeled the detail bands histograms by generalized Laplacian PDF (Probability Density Function)

$$p_X(x) = \exp\left(-\left|\frac{x}{s}\right|^p\right) \Big/ Z(s,p) \tag{1}$$

where s controls the width of the PDF and parameter p controls the shape. The $Z(s,p)$ function normalizes exponential to the unit area. The $Z(s,p)$ function is given by

$$Z(s,p) = \int_{-\infty}^{\infty} e^{-\left|\frac{x}{s}\right|^p} dx = 2\frac{s}{p}\cdot\Gamma\left(\frac{1}{p}\right) \tag{2}$$

where $\Gamma(x)$ presents the gamma function

$$\Gamma(x) = \int_0^{\infty} t^{x-1}e^{-t}dt. \tag{3}$$

4.2 Dark Frame Model

For the dark frame marginal PDF modeling the generalized Laplacian PDF was also utilized

$$p_N(x) = \frac{e^{-\left|\frac{x}{\beta}\right|^{\alpha}}}{Z(\alpha,\beta)} \tag{4}$$

where parameter α controls the shape of the PDF and parameter β controls the width.

5. Bayesian Estimators

The Bayesian statistics [7] has to be involved to one of the most powerful statistics methods. In comparison with the classical Fisher approach, the Bayesian approach

allows to subsume prior information to the problem solving. Since the Fisher approach utilizes only the observed data for the statistical problem solving, it is impossible to obtain useful results for a small number of data. The Bayesian approach provides useful results for a small set of obtained data because of the prior model usage. Two basic Bayesian estimators will be mentioned, Bayesian Least Square Error (BLSE) estimator, and Maximum a Posteriori (MAP) one.

5.1 Bayesian Least Square Error (BLSE)

Now the additive noise is assumed

$$y = x + n. \tag{5}$$

where x presents a clean signal, n stands for an additive noise and y is a noisy observation. It is generally known that the conditional mean of the posterior probability density function provides a least square estimation of the variable X. So the BLSE estimator should be written

$$\hat{X}(Y) = \frac{\int_{-\infty}^{+\infty} p_N(y-x)\cdot p_X(x)\cdot x\cdot dx}{\int_{-\infty}^{+\infty} p_N(y-x)\cdot p_X(x)\cdot dx}. \tag{6}$$

The denominator is the PDF of the noisy observation, computed via convolution of the signal and noise PDFs. The capital letters in PDF subscripts present variables in the wavelet domain.

5.2 Maximum a Posteriori (MAP)

So the additive noise is considered (5). The maximum a posteriori estimator is given by

$$\hat{X}(Y) = \arg\max_x p_N(y-x)\cdot p_X(x) \tag{7}$$

where p_N presents the noise PDF, p_X denotes the prior signal PDF.

5.3 Model Parameters Estimation Using Moment Method

The moment method, which is based on comparing of sample moments with theoretic moments, belongs to powerful parameters estimating methods.

Firstly it is necessary to derive theoretic moments for the random variable $Y = X + N$ ($E[X] = 0$, $E[N] = 0$) with several PDFs $p_X(X)$, $p_N(N)$ [8]. It can be shown that the second theoretic moment m_2 of Y will be only the addition of several generalized Laplacian moments

$$m_2(Y) = \frac{s^2\cdot\Gamma\left(\frac{3}{p}\right)}{\Gamma\left(\frac{1}{p}\right)} + \frac{\beta^2\cdot\Gamma\left(\frac{3}{\alpha}\right)}{\Gamma\left(\frac{1}{\alpha}\right)}. \tag{8}$$

The fourth theoretic moment m_4 of Y is given by

$$m_4(Y) = \frac{s^4\cdot\Gamma\left(\frac{5}{p}\right)}{\Gamma\left(\frac{1}{p}\right)} + \frac{6\cdot s^2\cdot\beta^2\cdot\Gamma\left(\frac{3}{p}\right)\cdot\Gamma\left(\frac{3}{\alpha}\right)}{\Gamma\left(\frac{1}{p}\right)\cdot\Gamma\left(\frac{1}{\alpha}\right)} + \frac{\beta^4\cdot\Gamma\left(\frac{5}{\alpha}\right)}{\Gamma\left(\frac{1}{\alpha}\right)}. \tag{9}$$

In accordance with [9] and [10], so-called kurtosis κ will be used, which is given by following expression

$$\kappa = \frac{m_4}{m_2^2} \tag{10}$$

where m_2 and m_4 denote the second and fourth theoretical moments. From the previous equations the following expressions can be derived

$$\kappa_X = \frac{\Gamma\left(\frac{1}{p}\right)\cdot\Gamma\left(\frac{5}{p}\right)}{\Gamma^2\left(\frac{3}{p}\right)}, \tag{11}$$

$$\kappa_X = \frac{m_4(Y) - m_4(N) - 6m_2(N)\cdot\left(m_2(Y) - m_2(N)\right)}{\left(m_2(Y) - m_2(N)\right)^2}, \tag{12}$$

$$s = \sqrt{\left(m_2(Y) - m_2(N)\right)\frac{\Gamma\left(\frac{1}{p}\right)}{\Gamma\left(\frac{3}{p}\right)}} \tag{13}$$

where $m_2(N)$ and $m_4(N)$ denote the second and fourth theoretic moment of N.

Equations (12) and (13) are still quite suboptimal, because the dark frame is not available and the moments $m_2(N)$ and $m_4(N)$ cannot be directly computed. Because of this, during the recent year, a set of dark frames has been acquired. For the dark frame acquiring, the astronomical camera SBIG ST-8 was used and image statistical analysis was done. The analysis has shown that the second and fourth sample moments are temperature dependent. Thence it follows that these dark frame moments in the wavelet domain should be found using the known moments temperature dependency. Now it is quite simple to estimate shape parameter α using kurtosis

$$\kappa_N = \frac{m_4(N)}{m_2^2(N)} = \frac{\Gamma\left(\frac{1}{\alpha}\right)\cdot\Gamma\left(\frac{5}{\alpha}\right)}{\Gamma^2\left(\frac{3}{\alpha}\right)}, \tag{14}$$

and β using the second moment

$$\beta = \sqrt{m_2(N)\frac{\Gamma\left(\frac{1}{\alpha}\right)}{\Gamma\left(\frac{3}{\alpha}\right)}}. \tag{15}$$

Practically all theoretical moments in equations (12), (13), (14) and (15) are replaced by the sample moments.

An example of optimization curve for parameter p (equation (14)) is depicted in Fig. 5 and the algorithm implementation can be seen in Fig. 6.

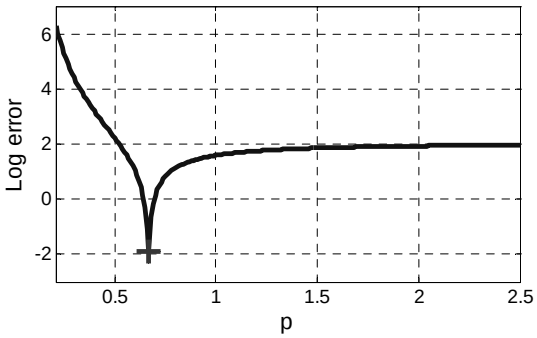

Fig. 5. Example of the optimization curve for parameter p, $M_2(N) = 7441$, $p = 0.67$.

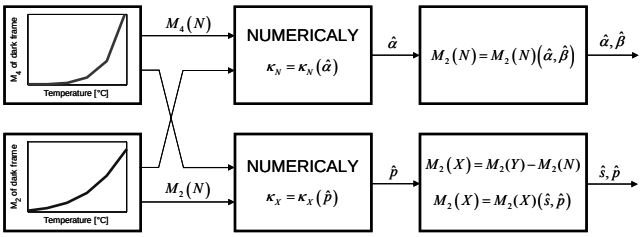

Fig. 6. The implementation of algorithm for parameters estimation.

5.4 Moments Temperature Dependency

This section closely investigates a temperature dependency especially of the second and fourth sample moment of the dark frame wavelet coefficients (dyadic decomposition, wavelet coiflet 4). Information about this temperature dependency is considerably essential, because there is no any other simple way how to estimate dark frame model parameters. The problem of the noise model parameters is not usually occurred in the case of additive Gaussian noise in multimedia images, because there exist many simple methods for noise variance estimation.

For the previous mentioned investigation of moments temperature dependency, the set of the dark frame images, which were acquired by the CCD camera SBIG ST-8 (CCD chip size 510 x 710 pixels), was used. The set of the dark frames contains 100 images at certain temperatures (-5, 0, 5, 10, 15, 20 °C). Because of the CCD camera temperature set accuracy, it is useless to choose finer temperature step than approx. 3°C. The exposure time was 60 seconds for all images. Fig. 7 shows the temperature dependency of the first sample moment of mean dark frames (spatial domain), which were obtained by averaging of 100 images acquired at several temperatures. This averaging process serves among others for the thermal noise (dark current fluctuation) suppression.

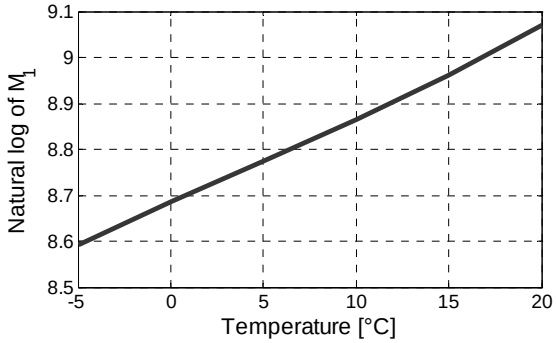

Fig. 7. Natural logarithm of the first sample moments (mean value) of the mean dark frames as a function of temperature, spatial domain.

Furthermore Fig. 7 well illustrates a linear temperature dependency of the natural logarithm of the first sample moments of the mean dark frames. From whence it follows that mean dark current has approximately exponential temperature dependency.

The following figures demonstrate temperature dependency of the second and fourth sample moments in the natural logarithm wavelet domain. The natural logarithm domain was utilized because of the considerably sample moments' varying.

There are the temperature dependencies of the second and fourth sample moments in Fig. 8 and 9. From these figures it can be concluded that the dark frames have similar moments in the wavelet domain at a certain decomposition level. When any uncorrected light image has to be corrected using the proposed Bayesian algorithm it is firstly crucial to assess the second and fourth sample moment value in accordance with the light image exposure time and temperature. So because of this the temperature moments curves have to be interpolated to obtain the moments value at non-measured temperatures.

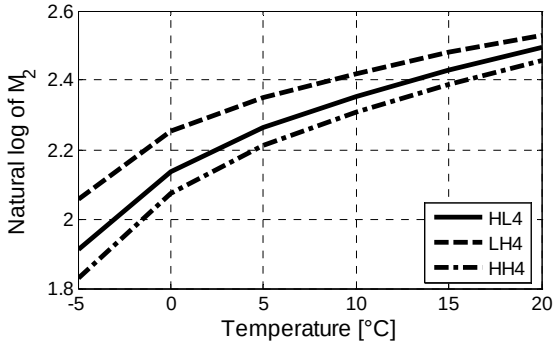

Fig. 8. Natural logarithm of the second sample moments of mean dark frames as a function of temperature, wavelet domain.

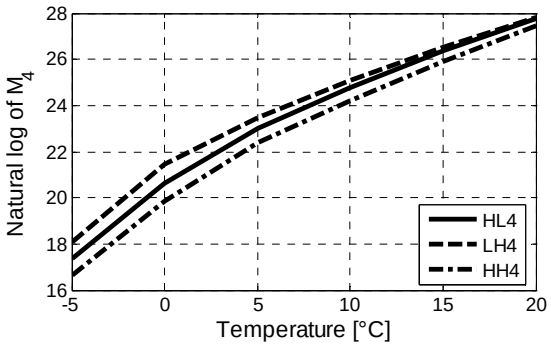

Fig. 9. Natural logarithm of the fourth sample moments of mean dark frames as a function of temperature, wavelet domain.

5.5 The Algorithm Implementation

The final algorithm implementation will be shown and explained here. There is the final algorithm implementation in Fig. 10.

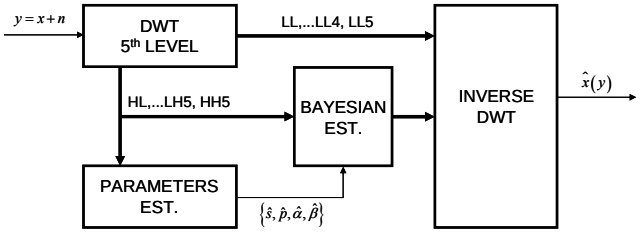

Fig. 10. The implementation of the thermally generated charge elimination algorithm.

The uncorrected image y is firstly decomposed to the fifth decomposition level (DWT or UWT can be used) then the model parameters are estimated using moment method (equations 11 to 15).

The estimated parameters are necessary for other processing in the Bayesian estimator (BLSE or MAP). For the final image reconstruction it is essential to apply inverse wavelet transform to the denoised detail subbands. All implementations were coded in the Matlab.

6. Results

In this section the results, which were obtained by the thermally generated charge elimination algorithm applied to astronomical data, will be discussed.

6.1 Aperture Photometry

Aperture photometry is based on pixel values integration in a certain area (called aperture) traced around a measured object. This method is practically independent of image quality. The problem may occur mainly in the case when a measured object laps an aperture.

There is an illustration of aperture photometry applied on the real light image in Fig. 11, where an annulus serves for the background measuring (subtracting) and a gap avoids a contamination of the sky annulus by a star. The aperture size is set as two or three times FWHM (Full Width at Half Maximum). Now it is good to note, which useful parameters can be computed in the aperture. The first parameter is a star magnitude, which is defined below.

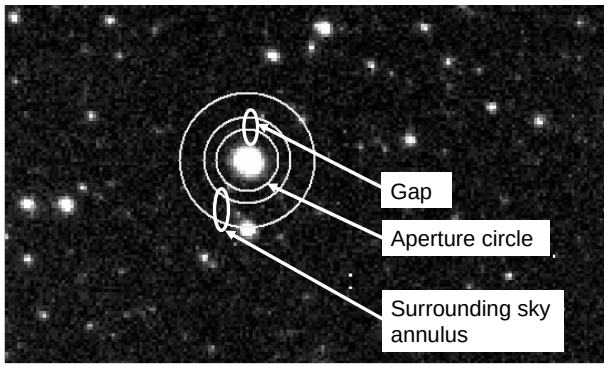

Fig. 11. Illustration of aperture photometry on real light image cut of 2g980831.006.fits.

A star magnitude tells us how bright the star is. Nowadays a magnitude is based on the Poggson equation, where the difference of the brightness of the two objects (measured and reference) is given by

$$mag_2 - mag_1 = -2.5 \log E_2/E_1 \tag{16}$$

where E_1 and E_2 denote the received flux power, mag_1 and mag_2 stand for the objects' magnitudes. Furthermore maximum and minimum pixel value, mean pixel value, standard deviation, FWHM etc. should be consequently evaluated in the aperture.

Now it is possible to start with aperture photometry. Firstly the chosen images were corrected by all combinations of Bayesian estimators (BLSE, MAP) and wavelet decompositions (DWT, UWT). The combination of MAP and UWT should not be utilized, because of time consumption. After that image sequence was made, where one of them represents three images (an image corrected by dark frame, an image corrected by Bayesian estimator, an image without any dark frame correction) given into one sequence image. In this sequence chosen stars were marked and star magnitude measurement was done. There is 3m42-d03.sbg.dat image in Fig. 12, where marked stars, which were measured, can be seen.

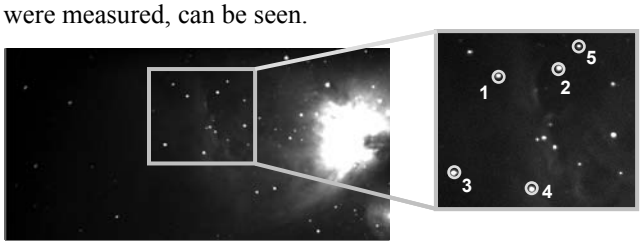

Fig. 12. The cut of 3m42-d03.sbg.dat image with the marked and numbered stars.

Tab. 1 and Tab. 2 summarize obtained star magnitudes, whereas *Mag ref* (was set to 10) denotes the reference star magnitudes (object 1-5 in the image corrected by the dark

frame), *Mag rough* stands for the magnitudes measured on the uncorrected image, *Mag measured* means magnitudes measured on the objects in the images corrected by several Bayesian estimators, *Δ Mag measured* equals to differences between *Mag ref* and *Mag measured*, *Δ Mag rough* equals to differences between *Mag ref* and *Mag rough*.

Object	Mag rough	Mag measured		
		BLSE		MAP
		DWT	UWT	DWT
Obj. 1	9.912	10.004	9.993	10.014
Obj. 2	9.962	10.053	9.951	10.131
Obj. 3	9.987	9.944	9.848	9.988
Obj. 4	9.989	10.014	9.865	10.080
Obj. 5	9.950	10.028	9.769	10.038

Tab. 1. The summary of star magnitudes measurement, the cut of 3m42-d03.sbg.dat.

Object	Mag rough	Δ Mag measured			Δ Mag rough
		BLSE		MAP	
		DWT	UWT	DWT	
Obj. 1	9.912	-0.004	0.007	-0.014	0.088
Obj. 2	9.962	-0.053	0.049	-0.131	0.038
Obj. 3	9.987	0.056	0.152	0.012	0.013
Obj. 4	9.989	-0.014	0.135	-0.080	0.011
Obj. 5	9.950	-0.028	0.231	-0.038	0.050

Tab. 2. The summary of star Δ magnitudes measurement, the cut of 3m42-d03.sbg.dat.

Summary of absolute value of *Δ mag measured* along with *Δ mag rough* is in Fig. 13. These dependencies illustrate an efficiency of the proposed algorithm. Obviously, if value of *Δ mag measured* is larger than *Δ mag rough* then the magnitude of the measured objects was measured better in the image corrected by Bayesian estimator.

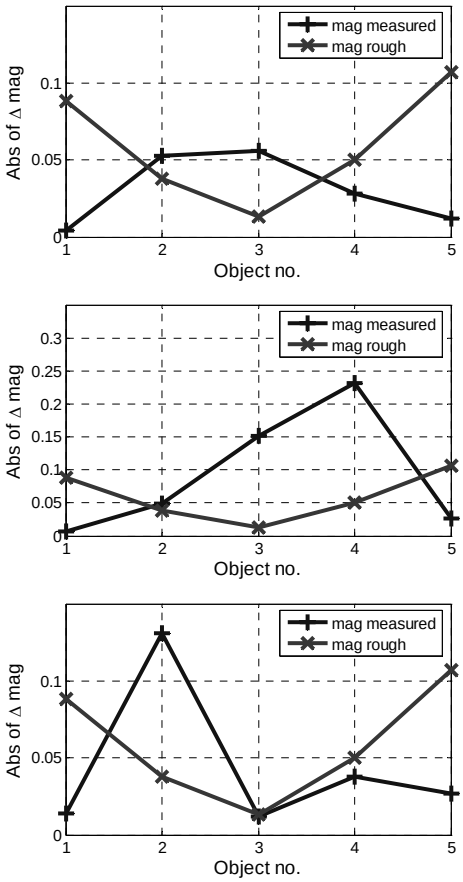

Fig. 13. The cut of 3m42-d03.sbg.dat, absolute value of *Δ mag measured* along with *Δ mag rough*, top - BLSE DWT, middle - BLSE UWT, bottom - MAP DWT.

7. Conclusion

The novel method for the thermally generated charge elimination was proposed. This method is based on the model of the light image and the dark frame in the wavelet domain. The equation system for the model parameters estimation was derived. The extensive measurement on the astronomical camera were proposed and done. After that the set of the astronomical testing images was corrected and then the objective criteria for image quality evaluation were applied. Objective criteria were based on aperture photometry. The photometry has shown that the proposed algorithm should be utilized for dark frame correction of various classes of astronomical images. Furthermore the algorithm considerably improves visual image quality, whereas fainter objects become visible and detectable.

Acknowledgements

The research described in the paper was financially supported by the research program MSM 6840770014.

References

[1] POSTIGO, A., SANGUINO, T. J., CERÓN, J. M., PÁTA, P., BERNAS, M. Recent developments in the BOOTES experiment. In *AIP Conf. Proc. 662*. Massachusetts Institute of Technology, 2003.

[2] MALLAT, S. G. A theory for multiresolution signal decomposition: the wavelet representation. *IEEE Transactions on Pattern Analysis and Machine Intelligence*, 1989, vol. 2, no. 7, p. 674–693.

[3] KOLZÖW, D. *Wavelets*. A tutorial and a bibliography, Erlangen, www: http://math.feld.cvut.cz/0educ/osn dokt-c/kolzow3.pdf

[4] ADAMS, N. *Denoising Using Wavelets*. www: http://www-personal.engin.umich.edu/~volafsso/Wavelet-Project/rep /DN.ps

[5] STARCK, J. L., FADILI, J. MURTAGH, F. The undecimated wavelet decomposition and its reconstruction. *IEEE Transaction on Image Processing*, 2007, vol. 16, no. 2, p. 297–309.

[6] SIMONCELLI, E. P. Bayesian denoising of visual images in the wavelet domain. In *Bayesian Inference in Wavelet Based Models*. Springer-Verlag, Lecture Notes in Statistics 141, 1999.

[7] ROWE, D. B. *Multivariate Bayesian Statistics: Models for Source Separation and Signal Unmixing*. Chapman and Hall/CRC, 2003.

[8] ŠVIHLÍK, J. Bayesian approach to the thermally generated charge elimination. In *Applications of Digital Image Processing XXX*. Bellingham, SPIE, 2007, p. 66961R-01-66961R-09.

[9] SIMONCELLI, E. P., ADELSON, E. H. Noise removal via Bayesian wavelet coring. In *Third Int'l Conference on Image Proc*. September 1996, vol. 1, p. 379 - 382, Lausanne. IEEE Signal Proc. Society.

[10] PIZURICA, A. *Image Denoising Using Wavelets and Spatial Context Modeling*. University Gent. 2002. PhD thesis.